Article

Discovery Medicine 2023; 35(178): 777–786
https://doi.org/10.24976/Discov.Med.202335178.72

Cepharanthine Inhibits Doxorubicin-Induced Cellular Senescence by Activating Autophagy via the mTOR Signaling Pathway

Jun Chen[1], Cheng Lei Xia[2], Rui Dong[1], Xian Guo Liu[3,*], Jing Xia[4,*]

[1]Department of Foot and Ankle Surgery, Chinese Medicine Hospital of Shizhong District of Leshan 12511002451599964Y, 614000 Leshan, Sichuan, China
[2]Department of Gynaecology, Leshan Hospital of Traditional Chinese Medicine, 614000 Leshan, Sichuan, China
[3]Department of Oncology, The Affiliated Chengdu 363 Hospital of Southwest Medical University, 610041 Chengdu, Sichuan, China
[4]School of Basic Medicine, Department of Human Anatomy Histology and Embryology, Dali University, 671000 Dali, Yunnan, China
*Correspondence: 18980792893@163.com (Xian Guo Liu); xxiajing@163.com (Jing Xia)
Published: 1 October 2023

Background: Doxorubicin (Dox) is a clinical first-line broad-spectrum anticancer agent. A dose-dependent cardiotoxic and myelosuppressive response limits the clinical use of Dox. Recent research indicates that Dox-induced cardiotoxicity is associated with senescent cell accumulation and that antiaging therapy can alleviate aging-related disorders. Cepharanthine (Cep) is commonly used to treat various acute and chronic illnesses, including leukopenia, snakebites, dry mouth, and hair loss. Whether Cep alleviates Dox-induced senescence is unknown.

Methods: The expression of genes and proteins associated with aging was examined using NIH3T3 cell lines. The experiments were divided into a control group, a Dox group, and a Cep group on different days. NIH3T3 senescent cells were detected by senescence-β-galactosidase (SA-β-Gal) staining, and Western blotting was used to detect the protein levels of p16, p53, AMP-activated protein kinase (AMPK), mammalian target of the rapamycin (mTOR), p62, and Light Chain 3 (LC3). Fluorescence was used to detect the expression of monomeric red fluorescence protein-green fluorescence protein-Light Chain 3 (mRFP-GFP-LC3) and LC3 puncta in NIH3T3 cells. Real-time quantitative reverse transcription polymerase chain reaction (RT–qPCR) was used to test the expression of senescence-associated secretory phenotypes (SASP: Interleukin 6 (IL-6), Interleukin 1 beta (IL-1β), and Interleukin 8 (IL-8)). Cell Counting Kit-8 (CCK-8) was used to assess NIH3T3 cell viability.

Results: Here, we reported that Cep reversed the Dox-induced increase in the proportion of SA-β-Gal-positive cells and the high expression of aging-related proteins (p53, $p < 0.05$; p16, $p < 0.05$) and aging-related genes (*IL-6*, $p < 0.05$; *IL-1*β, $p < 0.05$; *IL-8*, $p < 0.05$) on the 3rd day. Mechanistically, Cep reduced the increase in the levels of phospho-mTOR ($p < 0.05$) on Days 1 and 3 and p62 protein ($p < 0.05$) caused by Dox on Day 1 and reversed the decline in LC3II/LC3I levels ($p < 0.05$) caused by Dox on Day 3, which is associated with the regulation of senescence. Additionally, the viability of NIH3T3 cells was significantly increased in the concentration range of 0.5–5 µM Cep ($p < 0.05$).

Conclusions: We first found that Cep could suppress SA-β-Gal activity ($p < 0.05$) and the development of SASP. Additionally, in Cep-treated cells, Cep could restore autophagy dysfunction and suppress the mTOR signaling pathway. This research provides a new view on the mechanics of aging and autophagy and aids in developing novel antiaging drugs.

Keywords: Cepharanthine; Doxorubicin; senescence; autophagy; mTOR

Introduction

Doxorubicin (Dox) is an anthracycline anticancer drug widely used as a first-line chemotherapeutic drug for the treatment of various forms of cancer, such as breast cancer, osteosarcoma, and lymphoma [1]. Dox has restricted clinical application due to dose-dependent cardiotoxicity, myelosuppression (leukopenia, thrombocytopenia, anemia), and osteoporosis during administration. A cumulative dose of Dox higher than 400–700 mg/m^2 in adults and 300 mg/m^2 in children may dilate cardiomyocytes and cause cardiac failure. Many patients abandon Dox due to these severe side effects [2]. Dox-induced cardiotoxicity is primarily driven by oxidative stress, resulting in intracellular reactive oxygen species (ROS) and antioxidants being out of balance. Cellular senescence is an irreversible arrest of the cell cycle caused by a combination of factors such as oxidative stress, ultraviolet radiation, environmental pollution, and mitochondrial damage [3]. ROS are regarded as one cause of aging due to the molecular damage caused by oxidative stress. Mitochondria are the main targets of ROS damage, and their state is closely related to the senescence-associated secretory phenotypes (SASP)

[4]. As senescent cells accumulate, aging-related conditions may develop, such as cancer and blindness, as well as cardiovascular disorders. Hence, there is a need for antiaging drugs to treat diseases caused by aging.

Cepharanthine (Cep) has been widely used to treat radiotherapy-induced alopecia areata, leukopenia, and pityriasis alopecia since 1951 [5]. According to Rogosnitzky *et al*. [6], Cep has unique anti-inflammatory, antioxidant, antiparasitic, immunomodulatory, and antiviral properties. In recent years, to combat COVID-19 (SARS-CoV-2) caused by severe acute respiratory syndrome, Cep has shown remarkable antiviral effects, which has attracted attention from scholars worldwide [6]. However, the effectiveness of Cep in treating age-related conditions or its antiaging activity remains unclear. At the same time, in terms of preclinical research or clinical research, there is a lack of experimental data for the combined application of Dox and Cep.

Autophagy is a process of intracellular self-digestion that relies on highly conserved lysosomes [7]. In response to oxidative stress, hunger, and hypoxia, autophagy is usually low; however, research indicates that activation of autophagy can postpone the progression of Alzheimer's disease and treat age-related disorders. Conversely, inhibition of autophagy leads to many chronic conditions, such as cardiovascular and metabolic disorders [8]. Several studies have also demonstrated that mammalian target of the rapamycin (mTOR) signaling negatively regulates autophagy [9]. It has been reported that Dox causes cardiotoxicity and liver toxicity due to an accumulation of senescent cells by Feng *et al*. [10] and Aljobaily *et al*. [11]. In the future, the reduction in cellular senescence caused by Dox may be an option to alleviate its side effects.

The purpose of our study was to investigate the effect of Cep on Dox-induced cell senescence in NIH3T3 cells. Our experiments showed for the first time that Cep suppressed senescence-β-galactosidase (SA-β-Gal) activity and the increase in proinflammatory factors (Interleukin 6 (IL-6), Interleukin 1 beta (IL-1β), and Interleukin 8 (IL-8)) induced by Dox. This is the first study to show that Cep prevents Dox-induced senescence. We further found that Cep treatment inhibited the progression of Dox-induced premature senescence by activating autophagy. Cep also reduces aging by suppressing mTOR.

Materials and Methods

Cells and Reagents

NIH3T3 cells (Mouse embryonic fibroblast cells) were obtained from the Shanghai Institute of Biological Sciences, Chinese Academy of Sciences; Doxorubicin (S1208), Cep (S4238), and insulin (Ins) (S6955) were purchased from Selleck Shanghai Branch (Shanghai, China); Dulbecco Modified Eagle Medium (DMEM, E2107) was from Beijing Noble Ride Technology Co., Ltd. (Beijing, China); Chloroquine bisphosphonate (CQ) was obtained from Sigma-Aldrich (C6628, Carlsbad, California, USA); L-glutamic acid (CAS:56-86-0), 1% penicillin (P1400), and streptomycin (S8290) were obtained from Solarbio (Beijing, China); Cell Counting Kit-8 Kit (CCK-8, MA0218) was obtained from Dalian Meilun Biology (Dalian, Liaoning, China); Bicinchoninic Acid Assay (BCA) kit was from Solarbio (PC0020, Beijing, China); Antibodies against glyceraldehyde-3-phosphate dehydrogenase (GAPDH) were purchased from Abcam (Cat#ab181602, Cambridge, England). Anti-total mTOR recombinant rabbit monoclonal antibody [SU30-00] was purchased from HuaBio (ET1608-5, Hangzhou, Zhejiang, China). Phospho-mTOR (Ser2448) (Cat#5536), antibodies against Light Chain 3 (LC3) (Cat#12741), p53 (Cat# 2524), p16 (Cat#80772), p62 (Cat#5114), and phospho-AMP-activated protein kinase (p-AMPK) α (Thr172) (Cat#2536) were purchased from CST (Cell Signaling Technology, Boston, MA, USA); Anti-total AMPK rabbit polyclonal antibodies were purchased from ProteinTech Sangon Biotech (D221614, Shanghai, China). Peroxidase-conjugated goat anti-mouse immunoglobulin G (IgG) (H + L) and peroxidase-conjugated goat anti-rabbit IgG (H + L) were supplied by Proteintech China Co., Ltd. (A1101, A1108, Wuhan, Hubei, China).

Methods

Cell Culture

NIH3T3 (CL-0171) was obtained from the Wuhan Procell Life Science and Technology Co., Ltd. (Wuhan, Hubei, China). Mycoplasma testing has been performed. NIH3T3 cells were resuscitated and cultured in DMEM with 15% newborn calf serum and 2 mmol/mL L-glutamine in an incubator with 37 °C and 5% CO_2.

CCK-8 Cell Viability Assay

A suspension of 100 µL NIH3T3 cells (2.5×10^4/mL) was cultured for 24 hours in a 96-well plate. The culture medium was discarded, and a new complete medium was added. NIH3T3 cells were cocultured with 50 nmol/mL Dox and various concentrations of Cep (0.5–10 µM) for 3 days. Then, 10 µL of the CCK-8 reagent was added to 90 µL of DMEM, and the mixture was incubated for two hours. A Bio-Rad (iMark, Hercules, CA, USA) microplate spectrophotometer was used, and absorption was measured at 450 nm. Three replicates were conducted, and the average SD was calculated. Cell viability rate (%) = [(As – Ab)/(Ac – Ab)] × 100%. As, absorbance of the experimental group; Ac, absorbance of the control group; Ab, absorbance of the blank group.

SA-β-Gal Staining Experiments

The SA-β-Gal activity was assessed using the SA-β-Gal staining kit (G1508, Solebaol, Beijing, China) according to the manufacturer's instructions, and senescent

cells were identified as blue-green stained cells using phase contrast microscopy. The percentage of SA-β-Gal-positive cells in each group was determined by counting 1×10^3 cells in seven random fields. The experiment was repeated three times.

Compatibility of Drugs

Dox and Cep were dissolved in 100% dimethyl sulfoxide (DMSO, F8841, Solarbio, Beijing, China) at a concentration of 1×10^3 mmol/L in stock, stored at –20 °C, and diluted with the medium before each experiment. The concentration of DMSO used during the study never exceeded 0.1 percent (all control groups used 0.1% DMSO). A stock solution of chloroquine bisphosphonate and insulin was dissolved in DMSO to evaluate the effects of mTOR and autophagic activity regulators on Doxorubicin-treated senescent cells.

mRFP-GFP-LC3 Expression Cell Generation and Fluorescence LC3 Point Analysis

Cells were transfected with an monomeric red fluorescence protein-green fluorescence protein-Light Chain 3 (mRFP-GFP-LC3) plasmid (gt-ap-p101, Xingtuo Biotechnology, Shanghai, China), and G418 (ST081, Biyuntian Biotechnology Company, Changsha, Hunan, China), and G418 (Life Sciences, Berkeley, CA, USA) was used to select positive cells. Images of the intracellular distribution of LC3 were collected using an inverted fluorescence microscope, and red fluorescent protein (RFP) and green fluorescent protein (GFP) were fluorescently labeled. Mizushima *et al*. [12] used red and green puncta colocating macros in ImageJ (V1.8.0.112, NIH, Bethesda, MD, USA) to quantify the LC3-point material. Data were collected from more than 40 cells, and the number of LC3 points were counted. The experiment was repeated three times using yellow for GFP + RFP + puncta and red for GFP – RFP + puncta.

Western Blot Detection

We prepared a coldlysate from Mammalian cell-PE LBTM buffer (Organic buffer & 10 mM NaCl & detergent, pH 7.5) (GB-180, G-Biosciences & Geno Technology, St. Louis, MO, USA) containing phosphatase (Sigma-Aldrich, St. Louis, MO, USA). By mixing cells with ice-cold lysate for 30 min and centrifuging, NIH3T3 cell lysate is obtained. Protein concentration was detected using the BCA protein assay kit (71285-M, Sigma-Aldrich, St. Louis, MO, USA) method, and 2.5$\times$ Sodium Dodecyl Sulfate (SDS) loading buffer (Cat.No QYR1193, Qualityard, Beijing, China) was added to the lysate after 10 min of boiling. 25 µg protein was placed on an SDS-PAGE (Sodium Dodecyl Sulfate-Polyacrylamide Gel Electrophoresis) gel, subjected to 80 volts for 20 min, then adjusted to 120 volts for 1 hour to separate proteins of different molecular weights, and finally transferred to a polyvinylidene difluoride (PVDF) membrane (1620177, Bio-Rad, Hercules, CA, USA) by 150 mA electric current for 2-hours electrophoresis. The target protein was soaked in 5% skim milk for one hour and then incubated at room temperature with the primary antibody (1:1000), followed by the secondary antibody (1:10,000–1:100,000). Immune signals were detected using electrochemiluminescence methods, Super ECL Plus with Western blot reagent kits (TAN180-5001, FanZhi Biotechnology Company, Shanghai, China), and a Fusion Solo imaging system (UIm, Germany). Band intensity was quantified using ImageJ (V1.8.0.112, NIH, Bethesda, MD, USA) analysis software, and the experiment was repeated three times.

RT–qPCR Detection

In adherent NIH3T3 cells, total cellular RNA was extracted with TRIzol (Lot 03877, CWBIO, Beijing, China). The concentration of RNA was determined by an ultraviolet spectrophotometer (912A1024, NanoDrop, Thermo Scientific, Shanghai, China). The RNA concentration was measured in ng/µL. Complementary DNA (cDNA) was synthesized utilizing Moloney Murine Leukemia Virus Reverse Transcriptase (M-MLV) reverse transcriptase (M5301, Promega, Madison, WI, USA) from 1 µg total RNA. Amplification of the synthesized cDNA was performed using PCR. No genomic DNA was present in the samples. The synthesized cDNA was amplified using the HiScript II 1st Strand cDNA Synthesis Kit instructions (R211-01, Vazyme, Nanjing, China) using an ABI 7500 Fast Real-time PCR system (7500 Fast, Applied Biosystems, Carlsbad, CA, USA) with the HiScript II 1st Strand cDNA Synthesis Kit instructions (R211-01, Vazyme, Nanjing, Jiangsu, China). The reverse transcription condition: 50 °C for 15 min $\rightarrow$ 85 °C for 5 sec. Next, we used a real-time fluorescence quantitative PCR instrument (7900, ABI, Waltham, MA, USA), followed by the instruction procedure for real-time PCR using 2$\times$ SYBR Green qPCR Master Mix (Q712-02, Vazyme, Nanjing, Jiangsu, China). The sequences of the primers for RT–qPCR were as follows: *IL-1*β forward: F: 5′-TGGACCCCAGGATGAGGACA-3′ and reverse: R: 5′-TGGACCTTCCAGGATGAGGACA-3′; *IL-6* gene forward: F: 5′-ACTCACCTCTTCAGAACGAATTG-3′ and reverse: R: 5′-CCATCTTTGGAAGGTTCAGGTTG-3′; *IL-8* gene forward: F: 5′-CAAGGCTGGTCCATGCTCC-3′ and reverse: R: 5′-TGCTATCACTTCCTTTCTGTTGC-3′; *18s* gene forward: F: 5′-TTGACGGAGAGCACCAG-3′ and reverse: R: 5′-GCACCACCCACGGAATCG-3′. The experiment was repeated three times using the 18S ribosomal RNA sequences as an internal reference. The data were analyzed using Step One Software (v2.2, ABI, Waltham, MA, USA) to obtain the relative expression of genes. The $2^{-\Delta\Delta CT}$ method was used to calculate the expression of each gene associated with 18 sec.

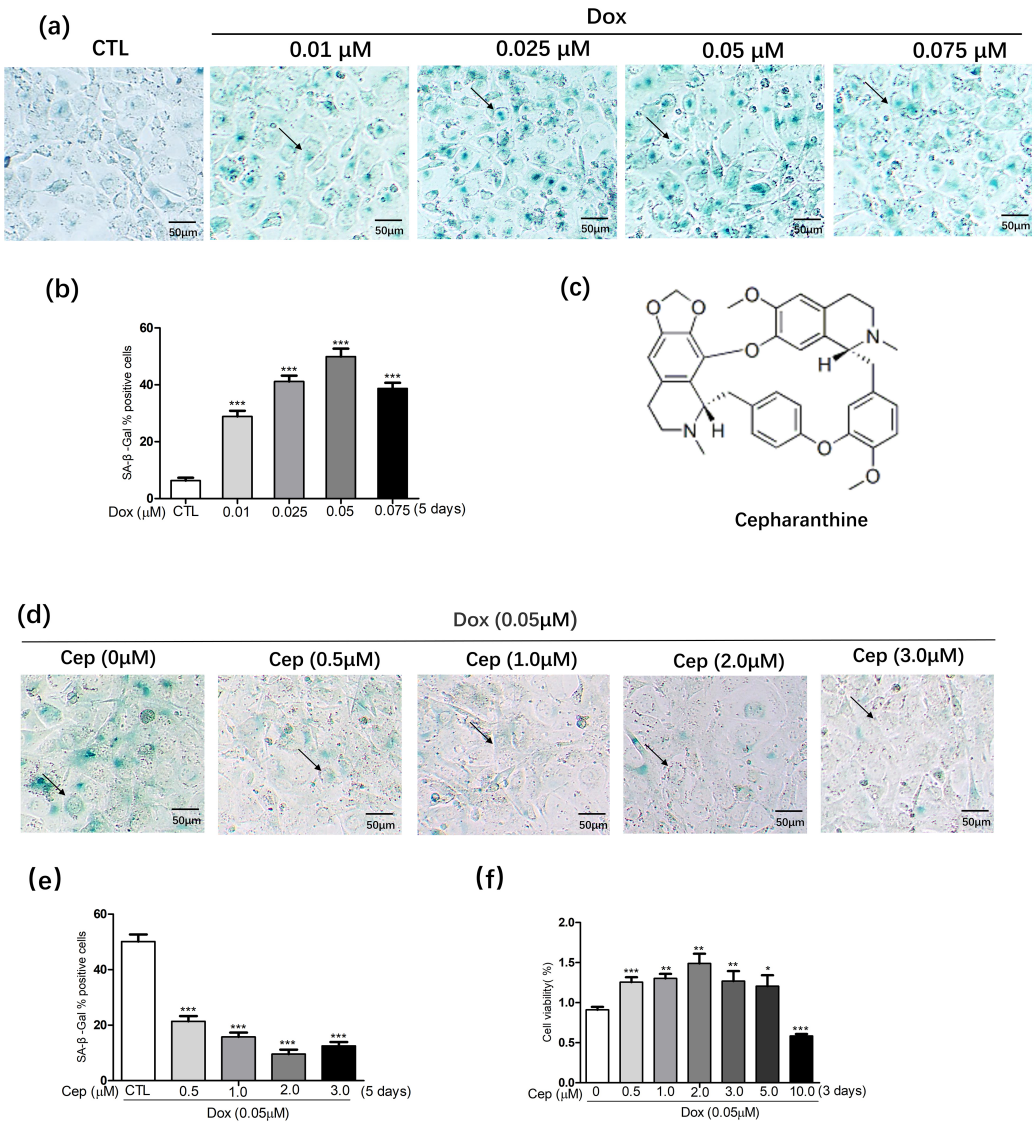

Fig. 1. Cepharanthine (Cep) inhibits Doxorubicin (Dox)-induced senescence-β-galactosidase (SA-β-Gal) activity in an NIH3T3 model. (a,b) Representative images and percent of SA-β-Gal-positive NIH3T3 cells treated with various concentrations of Dox (0.01 μM, 0.25 μM, 0.05 μM, and 0.075 μM) for 5 days. Scale bar: 50 μm. (c) The molecular structure of Cep. (d,e) Images and proportions of SA-β-Gal-positive NIH3T3 cells incubated with Dox (0.05 μM) or Cep plus Dox (0.5 to 3.0 μM) for 5 days. Scale bar: 50 μm. (f) NIH3T3 cells were treated with Dox (0.05 μM) plus Cep (0.3 to 10.0 μM) for 3 days; cell viability was measured by the Cell Counting Kit-8 Kit (CCK-8) reagent. *$p < 0.05$, **$p < 0.01$, and ***$p < 0.001$ versus the control (CTL) group.

Statistical Analysis

GraphPad Prism (Version 6.0, GraphPad Software Inc, San Diego, CA, USA) statistical software was used for statistical analysis. The measurement data are described as the mean ± SD, and one-way Analysis of Variance (ANOVA) was used to analyze the differences in multigroup means with Bonferroni post hoc tests. $p < 0.05$ is significant, and $p < 0.01$ is very significant.

Results

Cep Reduces the Increase in SA-β-Gal Activity Caused by Dox in NIH3T3 Cells

NIH3T3 cells are the most commonly used model cells for oxidative stress-induced premature senescence (SIPS) [13]. We referred to the dose of drug concentration in other literature, followed the results of the replicate pre-experiment, and then selected a safe concentration range suitable for cell experiments for subsequent experiments. As shown in Fig. 1a,b, different concentrations of Dox (0.01–0.75 μM) were added to NIH3T3 cells, followed by

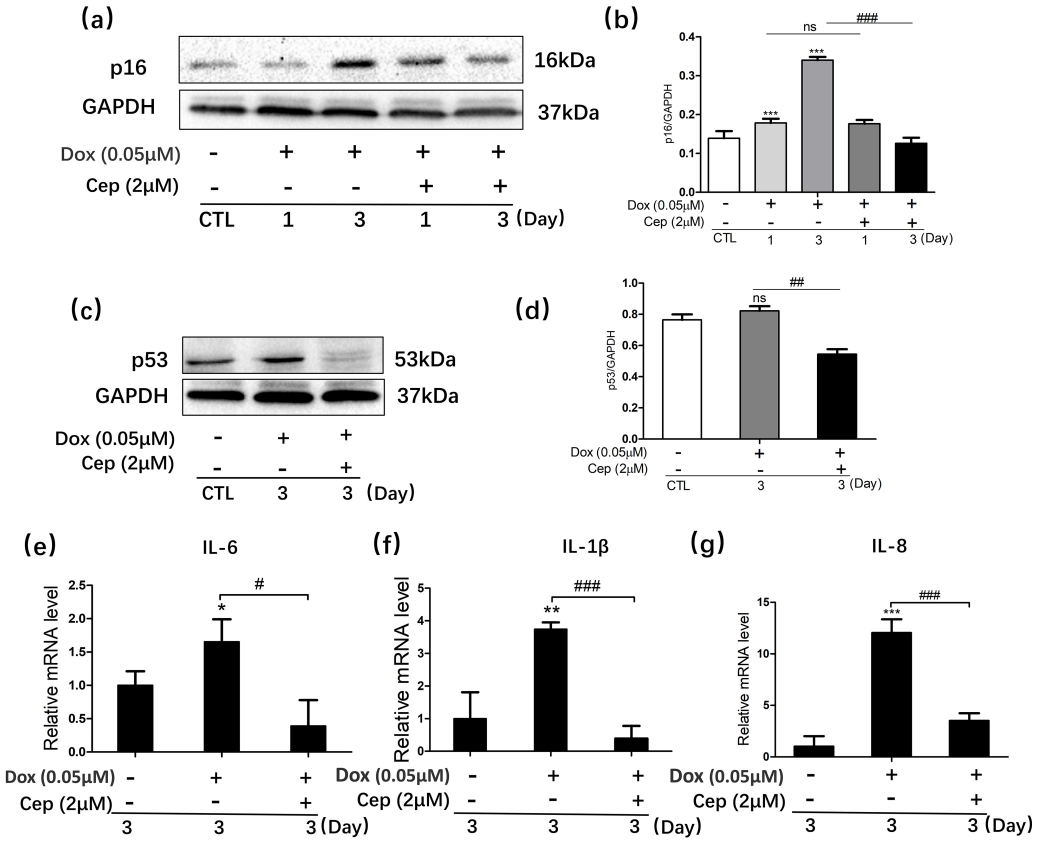

Fig. 2. The proportion of Dox-induced cell senescence is prevented by Cep. (a–d) Image of immunoblots and relative protein levels against p16, p53, and Glyceraldehyde-3-phosphate dehydrogenase (GAPDH). (e–g) Real-time quantitative reverse transcription polymerase chain reaction (RT–qPCR) was used to detect the relative mRNA levels (Interleukin 6 (*IL-6*), Interleukin 1 beta (*IL-1β*), and Interleukin 8 (*IL-8*)) of NIH3T3 cells treated with Dox (0.05 μM) and Dox plus Cep. The experimental data are presented as the means ± SEMs. n = 3. $*p < 0.05$, $**p < 0.01$, and $***p < 0.001$ versus CTL. $^{\#}p < 0.05$, $^{\#\#}p < 0.01$, and $^{\#\#\#}p < 0.001$ versus the indicated sample. "ns" is defined as not statistically significant. "–" represents no medicine; "+" represents medication.

solution change and culturing for five days, and then SA-β-Gal staining was performed. NIH3T3 cells became larger and flatter after Dox treatment. Moreover, SA-β-Gal staining was strongly positive. When the treatment concentration was 0.05 μM, the number of SA-β-Gal-positive cells reached more than 40% ($p < 0.05$). In subsequent experiments, we selected 0.05 μM Dox to treat cells. The current purpose of this study was to explore whether Cep can alleviate the toxic side effects of Dox. As shown in Fig. 1c–e, Cep significantly decreased the proportion of SA-β-Gal-positive cells, reaching 10%, and the antiaging effect was most obvious when the concentration of Cep was 1–2 μM (Fig. 1d,e). The viability of cells was also studied at different concentrations of Cep after Dox exposure. Compared with the Dox-treated group, Cep significantly increased the cell activity of NIH3T3 cells in the range of 0.5–5 μM (Fig. 1f, $p < 0.05$). Based on these results, we can conclude that Cep decreases the activity of SA-β-Gal induced by Dox.

Cep Reduces the Senescence-Related Protein and Gene Expression in NIH3T3 Cells Caused by Dox

In senescent cells, aging-related proteins (p16 and p53) are highly expressed, and many aging-related factors, including IL-6, IL-1β, and IL-8, are secreted [14]. Next, we detected the protein expression of p16 and p53 using Western blotting. Cep (2 μM) was chosen to treat cells. In Fig. 2a–d, p53 and p16 protein expression rose considerably in cells treated with Dox, especially on Day 3, while Cep significantly decreased the expression of p53 and p16 ($p < 0.05$). In addition, *IL-6*, *IL-1β*, and *IL-8* genes were detected using RT–qPCR. As shown in Fig. 2e–g, Cep significantly lowered the relative mRNA levels associated with senescence ($p < 0.05$). These results suggest that Cep can reduce the expression of NIH3T3 senescent cell-related proteins and genes.

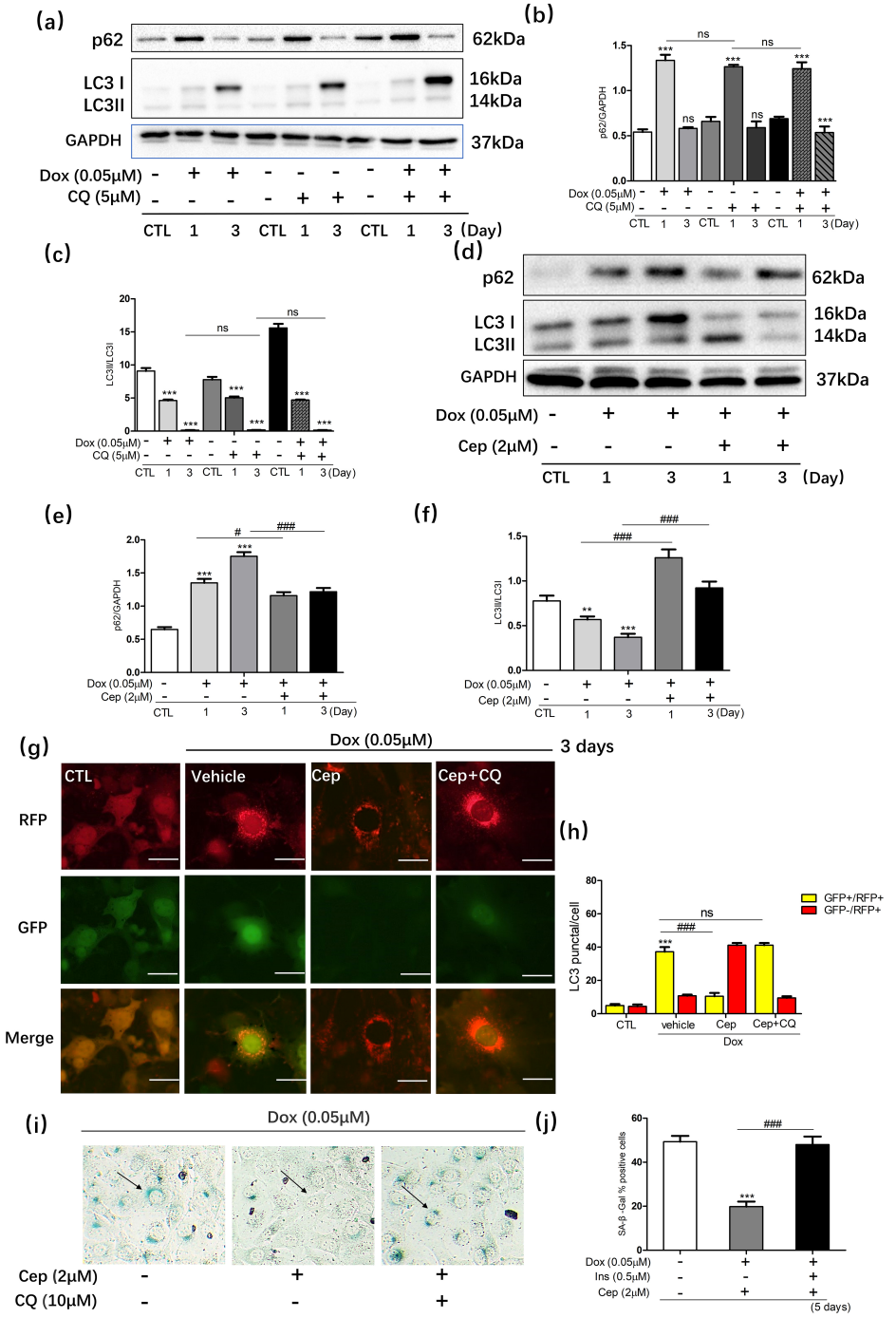

Fig. 3. Cep lessens the Dox-induced aging process by activating autophagy. Cells expressing red fluorescence protein-green fluorescence protein-Light Chain 3 (RFP-GFP-LC3) and NIH3T3 were incubated with different reagents for three days following Dox treatment, including vehicle, Cep (2 μM), and chloroquine bisphosphonate (CQ) (10 μM) in combination. (a) Images of immunoblots against p62 and Light Chain 3 (LC3). (b,c) Relative protein expression statistics (n = 3). (d) Representative images of Western blots against LC3 and p62. (e,f) Relative protein levels were quantified (n = 3). (g) The expression of RFP-GFP-LC3 cells; merged fluorescence is shown in the lower panel (200×). Scale bar: 50 μm. (h) In each treatment group, 30 randomly selected cells were counted to determine the number of puncta in each cell (g), divided into GFP + /RFP + and GFP – /RFP + groups. (i) Following Dox exposure, Cep alone or combined with CQ was applied to NIH3T3 cells for 5 days. Scale bar: 50 μm. (j) The percentage of SA-β-Gal-positive cells. $^{**}p < 0.01$, $^{***}p < 0.001$ versus the control group (CTL) or indicated sample. $^{\#}p < 0.05$, $^{\#\#\#}p < 0.001$ versus the indicated sample. "ns" is defined as not statistically significant. "–" represents no medicine; "+" represents medication; "vehicle" represents adding the same concentration of dimethyl sulfoxide (DMSO) but no medication.

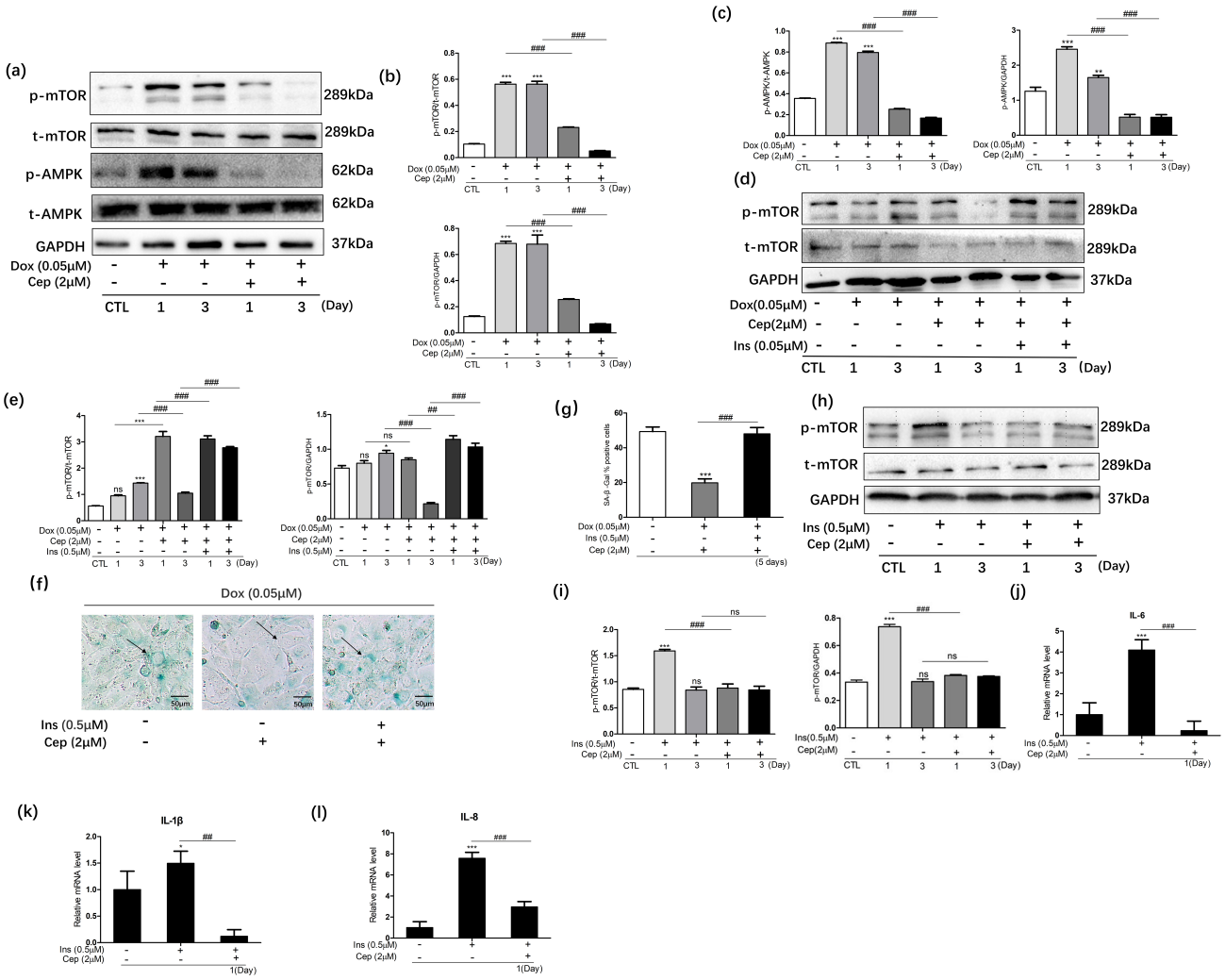

Fig. 4. Cep prevents Dox-induced senescence by inhibiting the mammalian target of the rapamycin (mTOR) pathway. (a) NIH3T3 cells were treated with Dox (0.05 μM) or Dox plus Cep (2 μM) for the 1st and 3rd days. Immunoblot images of phospho-mammalian target of the rapamycin (p-mTOR), total-mammalian target of the rapamycin (t-mTOR), phospho-AMP-activated protein kinase (p-AMPK), total-AMP-activated protein kinase (t-AMPK), and GAPDH. (b,c) Quantification of protein levels was performed (n = 3). (d) p-mTOR, t-mTOR and GAPDH immunoblot images. (e) Quantification of protein levels was performed (n = 3). (f,g) Images and ratios of SA-β-Gal-positive cells treated with Dox, Cep plus Dox, or Dox plus Cep plus insulin (Ins) for 5 days as indicated. Scale bar: 50 μm. (h) NIH3T3 cells were treated with insulin (0.5 μM) or Ins plus Cep (2 μM) for the 1st and 3rd days. Immunoblot images of p-mTOR, t-mTOR and GAPDH. (i) Quantification of protein levels were performed (n = 3). (j–l) RT–qPCR was used to detect the mRNA expression (IL-6, IL-1β, and IL-8) of NIH3T3 cells treated with Ins (0.5 μM) and Cep (2 μM). The experimental data are presented as the means ± SEMs. n = 3. *$p < 0.05$, **$p < 0.01$, ***$p < 0.001$ versus CTL. $^{\#\#}p < 0.01$, and $^{\#\#\#}p < 0.001$ versus the indicated sample. "ns" is defined as not statistically significant. "–" represents no medicine; "+" represents medication.

Cep Relieves Dox-Induced Cellular Senescence by Activating Autophagy

Autophagy and aging are closely linked; inhibiting autophagy leads to aging [15]. Western blotting was used to determine the levels of autophagy-related protein expression (p62 and LC3) in NIH3T3 senescent cells treated with Dox. The autophagy inhibitor chloroquine bisphosphonate (CQ) was used as a control. CQ inhibits autophagy by increasing the pH value of lysosomes, blocking autophagosome-lysosome binding, and inhibiting lysosomal decomposition. In NIH3T3 cells, p62 protein levels increased on Day 1, the ratio of LC3II/LC3I decreased with time, indicating that autophagy was inhibited, particularly when Dox was combined with CQ (Fig. 3a–c, $p < 0.05$). As shown in the above results, Dox and CQ exhibit similar autophagy inhibitory properties. When NIH3T3 cells were treated with Dox (0.05 μM), the protein expression level of p62 increased on Day 1 and decreased on Day 3, whereas the ratio of LC3II/LC3I decreased slightly on Day 1 and significantly on Day 3. Com-

pared with the Dox-treated group, the expression level of p62 protein was reduced, and the ratio of LC3II/LC3I was increased significantly when 2 μM Cep was added (Fig. 3d–f, $p < 0.05$). We can conclude that Cep activates Dox-inhibited autophagy. A tandem monomer RFP-GFP-tagged LC3 fusion protein was stably produced by NIH3T3 cells for the observation and differentiation of GFP + RFP + (yellow) and GFP – RFP + (red) LC3 punctate structures [15]. LC3 punctation, which is yellow, represents non-functioning autolysis and inactive autophagic fluxes, while LC3 punctation, which is red, indicates the opposite. Under Dox-induced oxidative stress, the red LC3 points of NIH3T3 cells gradually decreased, and the yellow LC3 points increased. Cep treatment decreased the number of yellow LC3 dots, and the dot color in the merged images tended to be GFP – RFP + (red). After combining with CQ, the dots in the merged image were GFP + RFP + (yellow). In other words, CQ significantly blocked the effect of Cep, which restored autophagic flux (Fig. 3g,h). As shown in Fig. 3i,j, CQ reversed the antiaging effect of Cep. The above experiments demonstrate that Cep can activate autophagy by altering autophagic flux, thus preventing aging.

Cep Alleviates Dox-Induced Cell Senescence in a Manner Dependent on the mTOR Signaling Pathway

In this study, we detected a pathway associated with autophagy regulation, the mammalian target of the rapamycin (mTOR) signaling pathway [16]. As shown in Fig. 4a,b, compared with the control group, Dox led to a gradual increase in mTOR phosphorylation levels with increasing days, especially on Day 3, and the expression level of phospho-mTOR protein increased significantly ($p < 0.05$). However, Cep combination treatment significantly reduced the protein level ($p < 0.01$) of p-mTOR on Days 1 and 3. As the literature describes, insulin is an mTOR-specific chemical activator [17]. Our experiments showed that the antiaging effect of Cep is closely related to mTOR signaling pathway inhibition. The mTOR activator insulin (Ins) reverted the mTOR phosphorylation level, which was inhibited by Cep (Fig. 4d,e, $p < 0.01$). Meanwhile, the addition of insulin considerably increased the ratio of SA-β-Gal-positive cells compared to the Cep group (Fig. 4f,g). We also found that Dox increased p-AMPK protein levels on Day 1 and Day 3 ($p < 0.01$), while Cep inhibited the increase in levels of the AMPK protein caused by Dox (Fig. 4a–c, $p < 0.01$); the causes for this were not addressed in this study. To further prove the antiaging effects of Cep, insulin significantly activated mTOR protein phosphorylation levels on the 1st day ($p < 0.01$), and then mTOR protein phosphorylation levels decreased because of the half-life of insulin on Day 3. During this period, the combination of Cep can still reduce the phosphorylation level of mTOR protein, an important node of the aging pathway (Fig. 4h,i, $p < 0.01$). Insulin leads to the occurrence of aging by activating the mTOR signaling pathway and meanwhile leads to an increase in the expression of age-related genes (*IL-6*, *IL-1*β, *IL-8*, $p < 0.05$), while the above experimental results were inhibited by Cep (Fig. 4j–l, $p < 0.01$). The results indicate that Cep can inhibit oxidative stress-induced aging.

Discussion

Cardiotoxicity and myelosuppression induced by Dox can be attributed to several different mechanisms, including the release of ROS, mitochondrial damage, lipid peroxidation, calcium overload, and lipid peroxidation [18]. *In vitro* experiments with Dox have demonstrated stress-induced premature aging of cells [19,20]. In our study, we found that Dox-induced a decrease in cell viability, proinflammatory cytokine release (IL-6, IL-1β, IL-8) and an increase in SA-β-Gal activity as well as aging-related proteins (p16, p53). These results are also confirmed by our experiments. Although numerous studies on humans and animals have proven the therapeutic effects of Cep against various human ailments, the close association between Doxorubicin-induced senescence and the alleviation of side effects remains unclear. Our results showed that Cep relieved the decrease in cell viability and the release of proinflammatory cytokine (IL-6, IL-1β, IL-8) caused by Dox. Meanwhile, Cep inhibited Dox-induced cell aging primarily by suppressing the mTOR signaling pathway and activating autophagy. Dox induces normal cell aging through mTOR signaling, which may also be one of the mechanisms of action behind cardiotoxicity and bone marrow suppression caused by Doxorubicin. The above data showed that Cep significantly relieved cellular senescence caused by Dox in NIH3T3 cells. This study identified a new therapeutic strategy for treating Dox toxicity with antiaging drugs.

Growing evidence indicates that mTOR plays a key role in autophagy and aging [21]. mTOR inhibitors, such as rapamycin, prevent oxidative stress-induced aging and activate autophagy by inhibiting mTOR [22,23]. In this study, we found that the antiaging effect of Cep was similar to that of rapamycin. We also observed that Cep delayed aging by activating autophagy; this further demonstrates that restoring autophagy can prevent senescence. We established a model of Dox-induced cellular senescence and found that aging led to the inhibition of autophagy activity, accompanied by autophagic flux damage. Our results are consistent with those of previous studies [24]. Aging is a complex process that accompanies age, decreased autophagy, and the consequent imbalance in protein balance and accumulation of protein toxicity, which ultimately leads to the development and/or progression of the disease [25]. Recently, autophagy has been shown to be activated in many long-lived biological models and to contribute significantly to longevity [26]. These results, combined with this study,

indicate that we can use old drugs with a new method and find similar Cep drugs by activating autophagy and inhibiting mTOR signaling pathways to delay aging.

Since its release in Japan, in addition to treating anemia, leukopenia, thrombocytopenia, alopecia, sarcoidosis, and some cancers, Cep has also been used to treat viral infection and human immunodeficiency virus (HIV) [27]. Some researchers have reported the therapeutic effects of Cep on dry mouth and snakebites. The mechanism of action of Cep involves multiple factors, including the interference of the cell membrane, metabolic axis (such as the NF-κB and JAK/STAT pathways), scavenging free radicals, combined with HsP90, and suppression by blocking autophagy of autophagy/lysosomal fusion mitochondrial autophagy [28]. Rongcan Luo *et al*. [29] found that upregulating autophagy could help treat diseases such as Alzheimer's disease. In metabolic disease, activation of autophagy may be a potential treatment for diabetic nephropathy [30]. Current research shows that Cep can slow oxidative stress by activating autophagy. However, at present, we have not used animal models and further animal experiments are needed to provide a theoretical basis for a detailed description of the molecular mechanisms involved in their action.

Conclusions

In conclusion, this study illustrates the inhibitory impact of Cep on Dox-induced aging. This possible mechanism is closely related to mTOR inhibition and autophagy activation. Our research offers a novel therapeutic strategy for managing Dox's side effects.

Abbreviations

AMPK, AMP-activated protein kinase; Cep, Cepharanthine; CTL, control; CQ, chloroquine bisphosphonate; Dox, Doxorubicin; PVDF, polyvinylidene difluoride; GFP, green fluorescent protein; HIV, human immunodeficiency virus; Ins, insulin; IL-1β, Interleukin 1 beta; IL-6, Interleukin-6; IL-8, Interleukin-8; mTOR, mammalian target of the rapamycin; RFP, red fluorescent protein; ROS, reactive oxygen species; SASP, senescence-associated secretory phenotypes.

Availability of Data and Materials

The data supporting the conclusions of this paper are included in the manuscript.

Author Contributions

JX, JC, and XGL designed the research study; JC performed the research; JC, RD, and CLX provided help and advice on the RT-qPCR fluorescence LC3 point analysis and WB experiments; JC and RD analyzed the data. All authors contributed to editorial changes in the manuscript. All authors read and approved the final manuscript. All authors have participated sufficiently in the work and agreed to be accountable for all aspects of the work.

Ethics Approval and Consent to Participate

Not applicable.

Acknowledgment

Not applicable.

Funding

The Innovative Scientific Research Project program for medical youth in Sichuan province (No.Q20074), the Project of medical research in Chengdu (NO.2021321), and the Le Shan City Key Research Project (Grant No.19SZD188) supported this manuscript.

Conflict of Interest

The authors declare no conflict of interest.

References

[1] Abdullah CS, Aishwarya R, Morshed M, Remex NS, Miriyala S, Panchatcharam M, *et al*. Monitoring Mitochondrial Morphology and Respiration in Doxorubicin-Induced Cardiomyopathy. Methods in Molecular Biology. 2022; 2497: 207–220.

[2] Songbo M, Lang H, Xinyong C, Bin X, Ping Z, Liang S. Oxidative stress injury in doxorubicin-induced cardiotoxicity. Toxicology Letters. 2019; 307: 41–48.

[3] Kumar R, Sharma A, Kumari A, Gulati A, Padwad Y, Sharma R. Epigallocatechin gallate suppresses premature senescence of preadipocytes by inhibition of PI3K/Akt/mTOR pathway and induces senescent cell death by regulation of Bax/Bcl-2 pathway. Biogerontology. 2019; 20: 171–189.

[4] Cardoso S, Seiça RM, Moreira PI. Uncoupling Protein 2 Inhibition Exacerbates Glucose Fluctuation-Mediated Neuronal Effects. Neurotoxicity Research. 2018; 33: 388–401.

[5] Rogosnitzky M, Danks R. Therapeutic potential of the bisoclaurine alkaloid, cepharanthine, for a range of clinical conditions. Pharmacological Reports. 2011; 63: 337–347.

[6] Rogosnitzky M, Okediji P, Koman I. Cepharanthine: a review of the antiviral potential of a Japanese-approved alopecia drug in COVID-19. Pharmacological Reports. 2020; 72: 1509–1516.

[7] Rajendran P, Alzahrani AM, Hanieh HN, Kumar SA, Ben Ammar R, Rengarajan T, *et al*. Autophagy and senescence: A new insight in selected human diseases. Journal of Cellular Physiology. 2019; 234: 21485–21492.

[8] Kaushik S, Tasset I, Arias E, Pampliega O, Wong E, Martinez-Vicente M, *et al*. Autophagy and the hallmarks of aging. Ageing Research Reviews. 2021; 72: 101468.

[9] Schmeisser K, Parker JA. Pleiotropic Effects of mTOR and Autophagy During Development and Aging. Frontiers in Cell and Developmental Biology. 2019; 7: 192.

[10] Feng M, Kim J, Field K, Reid C, Chatzistamou I, Shim M. Aspirin ameliorates the long-term adverse effects of doxorubicin through suppression of cellular senescence. FASEB BioAdvances. 2019; 1: 579–590.

[11] Aljobaily N, Viereckl MJ, Hydock DS, Aljobaily H, Wu TY,

Busekrus R, *et al*. Creatine Alleviates Doxorubicin-Induced Liver Damage by Inhibiting Liver Fibrosis, Inflammation, Oxidative Stress, and Cellular Senescence. Nutrients. 2020; 13: 41.

[12] Mizushima N, Yoshimori T, Levine B. Methods in mammalian autophagy research. Cell. 2010; 140: 313–326.

[13] Toussaint O, Medrano EE, von Zglinicki T. Cellular and molecular mechanisms of stress-induced premature senescence (SIPS) of human diploid fibroblasts and melanocytes. Experimental Gerontology. 2000; 35: 927–945.

[14] Rashidi S, Mansouri R, Ali-Hassanzadeh M, Mojtahedi Z, Shafiei R, Savardashtaki A, *et al*. The host mTOR pathway and parasitic diseases pathogenesis. Parasitology Research. 2021; 120: 1151–1166.

[15] Klionsky DJ, Abdelmohsen K, Abe A, Abedin MJ, Abeliovich H, Acevedo Arozena A, *et al*. Guidelines for the use and interpretation of assays for monitoring autophagy (3rd edition). Autophagy. 2016; 12: 1–222.

[16] Mendieta G, Ben-Aicha S, Casani L, Badimon L, Sabate M, Vilahur G. Molecular pathways involved in the cardioprotective effects of intravenous statin administration during ischemia. Basic Research in Cardiology. 2019; 115: 2.

[17] Zhang YM, Zimmer MA, Guardia T, Callahan SJ, Mondal C, Di Martino J, *et al*. Distant Insulin Signaling Regulates Vertebrate Pigmentation through the Sheddase Bace2. Developmental Cell. 2018; 45: 580–594.e7.

[18] Singh P, Sharma R, McElhanon K, Allen CD, Megyesi JK, Beneš H, *et al*. Sulforaphane protects the heart from doxorubicin-induced toxicity. Free Radical Biology & Medicine. 2015; 86: 90–101.

[19] Li D, Yang Y, Wang S, He X, Liu M, Bai B, *et al*. Role of acetylation in doxorubicin-induced cardiotoxicity. Redox Biology. 2021; 46: 102089.

[20] Huang P, Bai L, Liu L, Fu J, Wu K, Liu H, *et al*. Redd1 knockdown prevents doxorubicin-induced cardiac senescence. Aging. 2021; 13: 13788–13806.

[21] Wang X, Wang XL, Chen HL, Wu D, Chen JX, Wang XX, *et al*. Ghrelin inhibits doxorubicin cardiotoxicity by inhibiting excessive autophagy through AMPK and p38-MAPK. Biochemical Pharmacology. 2014; 88: 334–350.

[22] Zhuo L, Cai G, Liu F, Fu B, Liu W, Hong Q, *et al*. Expression and mechanism of mammalian target of rapamycin in age-related renal cell senescence and organ aging. Mechanisms of Ageing and Development. 2009; 130: 700–708.

[23] Zhang Y, Zhang J, Wang S. The Role of Rapamycin in Healthspan Extension via the Delay of Organ Aging. Ageing Research Reviews. 2021; 70: 101376.

[24] Nakamura S, Oba M, Suzuki M, Takahashi A, Yamamuro T, Fujiwara M, *et al*. Suppression of autophagic activity by Rubicon is a signature of aging. Nature Communications. 2019; 10: 847.

[25] Carmona-Gutierrez D, Hughes AL, Madeo F, Ruckenstuhl C. The crucial impact of lysosomes in aging and longevity. Ageing Research Reviews. 2016; 32: 2–12.

[26] Sun J, Cheng B, Su Y, Li M, Ma S, Zhang Y, *et al*. The Potential Role of m6A RNA Methylation in the Aging Process and Aging-Associated Diseases. Frontiers in Genetics. 2022; 13: 869950.

[27] Huang H, Hu G, Wang C, Xu H, Chen X, Qian A. Cepharanthine, an alkaloid from Stephania cepharantha Hayata, inhibits the inflammatory response in the RAW264.7 cell and mouse models. Inflammation. 2014; 37: 235–246.

[28] Bailly C. Cepharanthine: An update of its mode of action, pharmacological properties and medical applications. Phytomedicine. 2019; 62: 152956.

[29] Luo R, Su LY, Li G, Yang J, Liu Q, Yang LX, *et al*. Activation of PPARA-mediated autophagy reduces Alzheimer disease-like pathology and cognitive decline in a murine model. Autophagy. 2020; 16: 52–69.

[30] Liu WJ, Huang WF, Ye L, Chen RH, Yang C, Wu HL, *et al*. The activity and role of autophagy in the pathogenesis of diabetic nephropathy. European Review for Medical and Pharmacological Sciences. 2018; 22: 3182–3189.